Article

A Dual Fluorometric and Colorimetric Sulfide Sensor Based on Coordinating Self-Assembled Nanorods: Applicable for Monitoring Meat Spoilage

Rana Dalapati, Matthew Hunter and Ling Zang *

Department of Materials Science and Engineering, Nano Institute of Utah, University of Utah,
Salt Lake City, UT 84112, USA
* Correspondence: lzang@eng.utah.edu

Abstract: Psychrotrophic bacteria, commonly called spoilage bacteria, can produce highly toxic hydrogen sulfide (H_2S) in meat products. Thus, monitoring the presence of hydrogen sulfide in meat samples is crucial for food safety and storage. Here, we report a unique chemical sensor based on supramolecular nanorods synthesized via copper ion induced self-assembly of *N,N*-bis[aspartic potassium salt]-3,4,9,10-perylenetetracarboxylic diimide (APBI-K). The self-assembled nanorods can specifically detect sulfide with a detection limit of 0.181 μM in solution. The nanorods suspended in pure water show a turn-on fluorescence sensing behavior along with color change, acting as a dual fluorometric and colorimetric sensor. Spectroscopic investigation confirms the sensing mechanism due to copper ion displacement induced by the association with sulfide. Based on the high selectivity and sensitivity, supramolecular nanorod sensors were successfully employed to detect H_2S in spoiled meat sample as well as dissolved H_2S in water.

Keywords: perylene tetracarboxylic dimide; metal induced self-assembly; self-assembled nanorod; H_2S sensor; fluorescence sensor; meat spoilage; food safety

1. Introduction

Hydrogen sulfide (H_2S), being nearly as toxic as carbon monoxide gas, can cause severe health damage and even death [1]. The endogenous H_2S is primarily produced by enzyme-catalyzed reactions from various sulfur-containing amino acids which include cysteine, homocysteine, and methionine in the metabolic pathway [2]. Under standard conditions, 70% of H_2S is generated from cysteine and the residual 30% is produced from homocysteine [3]. Highly water soluble H_2S exists primarily in three different forms, namely: S^{2-}, HS^- and H_2S. The form of the sulfide is dependent on the pH of the aqueous medium [4,5]. Serious physiological problems, like Down syndrome [6], diabetes [7], liver cirrhosis [8], and Alzheimer's [9], can arise from excess sulfide exposure. In addition to the industrial sources of H_2S, the illegal use of sulfide additives in food such as sulfites, rongalite, and sodium sulfide can cause harmful effects on human health [10]. Nevertheless, sulfide is overly formed in the process of food rot. Meat and meat-based foods are very susceptible to spoilage. The Gram-negative bacteria, *Shewanella putrefaciens*, and *Citrobacter freundii* present in meat can be active at low temperatures and can rapidly produce sulfides when growing [11,12]. Thus, sulfide can act as a marker of meat spoilage. According to the World Health Organization (WHO), food containing harmful bacteria, pathogens, viruses, parasites, or toxic chemical additives cause more than 200 different diseases in humans [13]. Detection of sulfides in food is still a challenging task because of the complexity of food compositions and the presence of interfering ingredients. Thus, a sensitive and effective sulfide detection method is in great demand to ensure food safety and human health.

Several traditional detection techniques such as chromatographic assays [14,15], electrochemical analysis [16,17], metal-oxide–semiconductor-based electronic nose [18,19], and

visible light colorimetric technology [20,21] have been employed for detecting levels of sulfides. However, most detection techniques are time-consuming and need to be conducted in specialized laboratory settings by highly trained individuals. Spoilage of food, especially meat, is very time dependent. Because of this, on-site detection of sulfides by simple instrumentation is highly desirable for real-time monitoring of food substrates. In recent years, naked-eye detection of sulfides, using either colorimetric or fluorometric probes, got enormous attention from the scientific community due to its simplicity, high selectivity, sensitivity, and fast response time [22–29]. An ideal sensor should feature fluorescence turn-on performance, fast response time, high sensitivity, and selectivity over interfering components. A color change with target analyte exposure is also desired. Unfortunately, a large number of sensors work only in pure organic solvents or in mixed aqueous solvents [2,30–32]. The use of toxic organic solvents restricts the materials' applications as useful sensors in the field, especially in a food industry setting. Therefore, the development of a simple sensing platform that can detect sulfide contamination on-site without using complex instrumentation is still necessary.

Herein, we report a new, dual fluorometric and colorimetric probe using nanorods made by the coordination induced self-assembly of Cu^{2+} ion and *N,N*-bis[aspartic potassium salt]-3,4,9,10-perylenetetracarboxylic diimide (APBI-K) [33]. The potassium salt of tetracarboxylic acid increases the water solubility of the perylene diimide (PDI) core and helps nanorods assemble via rapid complex formation with Cu^{2+} ion. These coordinating self-assembled nanorods (**APBI-Cu**) were made by mixing the aqueous solutions of $Cu(NO_3)_2$ and APBI-K. Spectroscopic investigation suggests that **APBI-Cu** nanorods were formed via intermolecular intrinsic π-π stacking driven by Cu^{2+}-APBI-K complexation accompanied by fluorescence quenching. Sulfides have a strong binding affinity for Cu^{2+} ions, consistent with the extremely low solubility product constant of CuS, 7.9×10^{-37} [34]. Thus, Cu^{2+} present in nanorods acts as an active metal center towards sulfides. The presence of sulfide ions triggers the competitive binding with the Cu^{2+} ion, resulting in the disassembly of **APBI-Cu** nanorods. Consequently, in the presence of Na_2S (commercially available H_2S donor) [35], a turn-on fluorometric and colorimetric response from **APBI-Cu** nanorods was observed.

2. Materials and Methods

2.1. Materials and Instrumentations

N,N-bis[aspartic potassium salt]-3,4,9,10-perylenetetracarboxylic diimide (APBI-K) was synthesized by following a previously published procedure [33]. Reagent grade starting materials were used as received from the commercial suppliers. Ultrapure Milli-Q water (Millipore) was used during all experiments. Fresh chicken mince was acquired from a local market (Salt Lake City, UT, USA).

UV–Vis spectra were obtained by using an Agilent Cary 100 spectrophotometer. Emission spectra were recorded by using an Agilent Cary Eclipse fluorescence spectrophotometer. Attenuated total reflectance-infrared (ATR-IR) spectra were measured on a Nicolet iS50 FTIR Spectrometer at room temperature. Scanning electron microscopy (SEM) images were obtained on the FEI Nova NanoSEM™ scanning electron microscope. ^{1}H NMR spectrums were carried out on a Varian Mercury 400 MHz spectrometer.

2.2. Synthesis of APBI-Cu Nanorods

An aqueous solution of $Cu(NO_3)_2$ (2 mL, 10 mM) was slowly mixed with an aqueous solution of APBI-K (2 mL, 1 mM). The mixture was aged overnight to complete the self-assembly process. The nanorods were collected by centrifugation, washed thoroughly with water and dried in an air oven. Dried samples were used for experimentation.

2.3. Fluorescence Sensing Experiment in Water

5 mg **APBI-Cu** nanorods were dispersed in water by sonication. 50 μL of **APBI-Cu** nanorod suspension was diluted in 2 mL water. Fluorescence emission was monitored

at 547 nm, using an excitation wavelength of 490 nm upon incremental addition of Na_2S solution. Similar experiments were carried out by substituting Na_2S with other interfering analytes. The sensitivity was examined by adding 100 μM of Na_2S to the nanorod suspension containing other interfering analytes.

For paper-based test-strip fabrication, 10 cm × 10 cm clean Whatman filter papers were immersed in 1 mM aqueous solution of APBI-K solution. The paper was dried in an oven and then immersed in 10 mM aqueous solution of $Cu(NO_3)_2$. Then, the paper was washed with water to remove the loosely bound complex on the surface. The **APBI-Cu** coated paper was dried under vacuum and stored in a dark environment prior to use.

2.4. Detection of Sulfide in Chicken Sample

Fresh chicken mince (~5 g) was placed in two separate 250 mL round bottom flasks and sealed with septa. One flask was kept refrigerated at −4 °C and the other was kept at room temperature (~25 °C). Gas was collected from the headspace of the round bottom flask using a 25 mL syringe with 24 h intervals. The collected gas was then slowly bubbled in the aqueous suspension of **APBI-Cu** nanorods.

3. Results and Discussions

3.1. Design and Synthesis of APBI-Cu Nanorods

The designed fluorophore molecule, APBI-K, is highly water soluble due to its salt form (Scheme 1). Such high-water solubility is essential for the sensor to be used in a pure water system. The optical properties of free APBI-K were studied by measuring absorption and emission spectra in water at room temperature. As shown in Figure 1, the normalized spectra of APBI-K show two strong absorption bands near 532 nm, 495 nm along with a broad shoulder peak around 465 nm. This typical characteristic absorbance could be assigned to the 0–0, 0–1, and 0–2 transition energy [36–38]. The emission spectra of the same solution portray the similar structural features with nearly mirror images of the absorption spectra, and the emission peaks appear at 547 nm, 587 nm, and a weak shoulder peak near 638 nm.
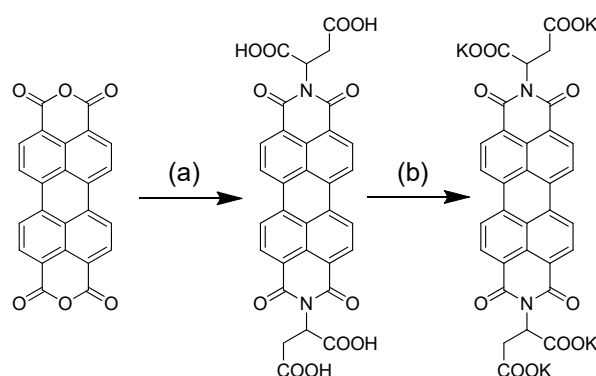
Scheme 1. Synthesis pathway of APBI-K. (**a**) DL-Aspartic Acid, imidazole, N_2 atm., 6 h, 120 °C. (**b**) KOH (excess), H_2O.

Coordination induced self-assembly was studied by using aqueous solutions of APBI-K and $Cu(NO_3)_2$. When Cu^{2+} was introduced into the APBI-K solution at a 10:1 molar ratio, a rapid precipitate formation was observed, which confirms the water-soluble fluorophore molecules undergo a fast coordination complex formation with Cu^{2+} ion. A clear supernatant solution was observed after standing overnight, confirming the completion of the process (Figure 2a,b). The SEM imaging confirms the nanorod morphology of the self-assembled **APBI-Cu** precipitates (Figure 2c,d). Another set of self-assembled precipitates was obtained from the same APBI-K solution by evaporating the solution without adding any Cu^{2+} ion solution. No distinct morphology was found for only APBI-K material

(Figure S1, Supplementary Materials). This result suggests that Cu^{2+} ion coordination is important to obtain monodispersed nanorods.
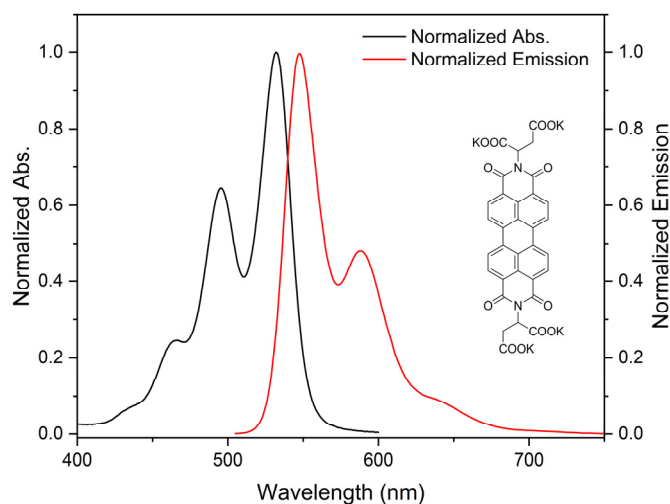

Figure 1. Normalized absorption and emission spectra of APBI-K in water. Inset: Chemical structure of APBI-K molecule.
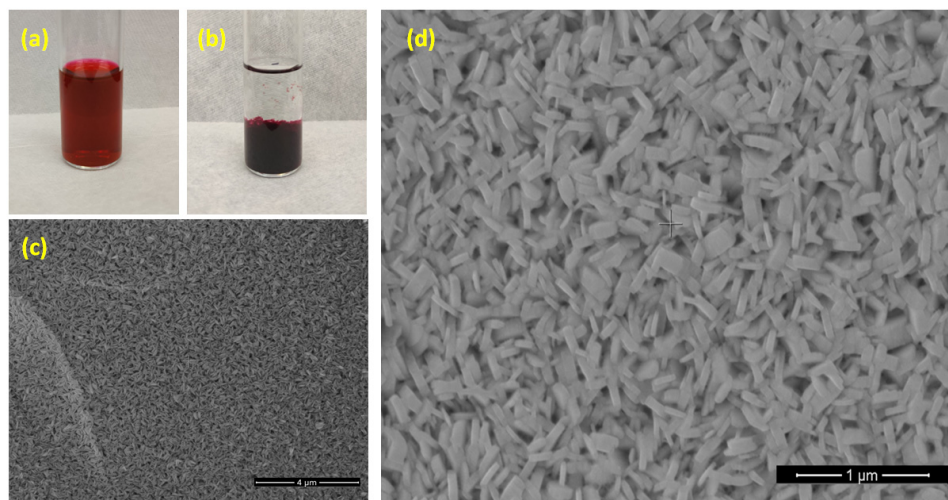

Figure 2. (**a**) The digital image of the 1 mM **APBI-K** aqueous solution. (**b**) The digital image of the nanorod synthesized by addition of $Cu(NO_3)_2$ into the aqueous solution of **APBI-K**. (**c**) SEM image of the **APBI-Cu** nanorods. (**d**) Enlarged SEM image of **APBI-Cu** nanorods.

Copper coordinating self-assembly was further investigated spectroscopically. A 10:1 equivalent of Cu^{2+} ion was incrementally added in APBI-K solution, and both absorption and emission spectral changes were monitored. The aqueous solution of APBI-K shows the absorption ratio of 0–0 and 0–1 band (A_{0-0}/A_{0-1}) as nearly 1.52 (Figure 3a). It is worth mentioning that the A_{0-0}/A_{0-1} ratio obtained from absorption spectra is considered a tool to monitor the aggregation behavior of perylene diimides (PDIs). Franck-Condon progression with a ratio A_{0-0}/A_{0-1} of ~1.6 is considered for free monomeric PDIs [39]. Thus, APBI-K solution primarily exists in monomeric form in solution. The ratio of A_{0-0}/A_{0-1} changed rapidly with the addition of Cu^{2+} and shows A_{0-0}/A_{0-1} value of ~0.94. This result indicates the formation of an aggregated state in the presence of Cu^{2+} ion [40]. A new broad shoulder near 570 nm was also observed with increasing Cu^{2+}, which also suggests the formation of a new species via coordinating self-assembly of APBI-K molecules [41,42]. A clear isosbestic point was observed at 550 nm, indicating quantitative conversion of APBI-K

from free molecular state to the aggregate. The emission behavior of nanorods is also drastically different compared to the free APBI-K molecules (Figure 3b). A 98% quenching was observed upon formation of a self-assembled compound. These results suggest that the addition of Cu^{2+} ions boost the π-π stacking among PDI core and facilitates the formation of coordinating self-assembled nanorods.
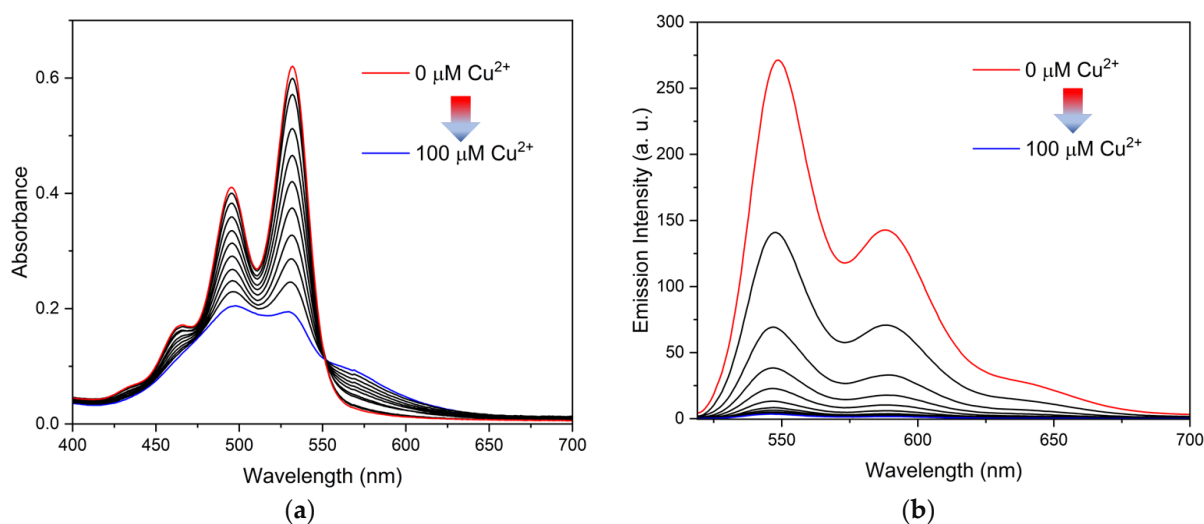

Figure 3. The change in absorption (**a**) and emission spectra (**b**) of **APBI-K** aqueous solution during formation of coordination induced self-assembly with incremental addition of Cu^{2+} ion.

To obtain further structural information of **APBI-Cu** nanorods, ATR-IR spectra were also recorded (Figure S2, Supplementary Materials). Free APBI-K displays strong absorption bands in the areas of 1570 and 1343 cm^{-1}. These bands can be assigned to the asymmetric and symmetric CO_2 stretching vibrations of the potassium coordinated APBI-K fluorophore [33,43]. The peak corresponding to CO_2 stretching vibrations diminished in intensity and broadened upon nanorod formation. This result validates the coordination bond formation between Cu^{2+} and APBI-K via the carboxylate functional group during self-assembly [44,45].

3.2. Detection of Sulfide in Water

It is well known that copper has stronger affinity to sulfides compared to carboxylates [46,47], consistent with the dramatically different solubility product constants of CuS (7.9×10^{-37}) and $CuCO_3$ (1.4×10^{-10}) [34,48]. Based on this metal ion displacement approach (MDA), various colorimetric and fluorometric probes have been reported [2,30,49–55]. However, the use of perylene diimide (PDI) based metal coordinated self-assembled materials as a sulfide sensor is rare. Recently, Yao et al. reported H_2S sensing using a similar mechanism with a 0.41 μM detection limit [53]. However, the use of highly toxic cadmium metal could restrict the sensor application in real world applications. Thus, the self-assembled **APBI-Cu** nanorods could be a better option for sulfide sensing considering their real-world application potential.

To test the sulfide sensing ability of **APBI-Cu** nanorods, the nanorods were dispersed in water and an aqueous solution of Na_2S was added incrementally. As depicted in Figure 4a, a rapid turn-on fluorescence signal was observed in the presence of sulfide in the system. The spectral pattern is the exact same as free APBI-K molecules. A time-dependent study shows that the turn-on signal gets saturated within 120 s (Figure S3, Supplementary Materials). Such a fast response is desirable for rapid onsite sensor development. In the presence of sulfide, the color of the solution also changes to red with the reappearance of typical 0–0 and 0–1 transition peaks in UV-Vis spectra (Figure S4, Supplementary Materials). A change of pH was also observed during the sensing experiments. The pH of the system

changes from 5.4 to 7.8. Thus, to stabilize the pH of the system, a same experiment was carried out in 10 mM HEPES buffer at pH 7.4. As shown in Figure S5, **APBI-Cu** nanorods can detect the sulfide in buffer medium efficiently. Hence, the spectral study in both water and buffer medium confirm the sulfide sensing ability of **APBI-Cu** nanorods.
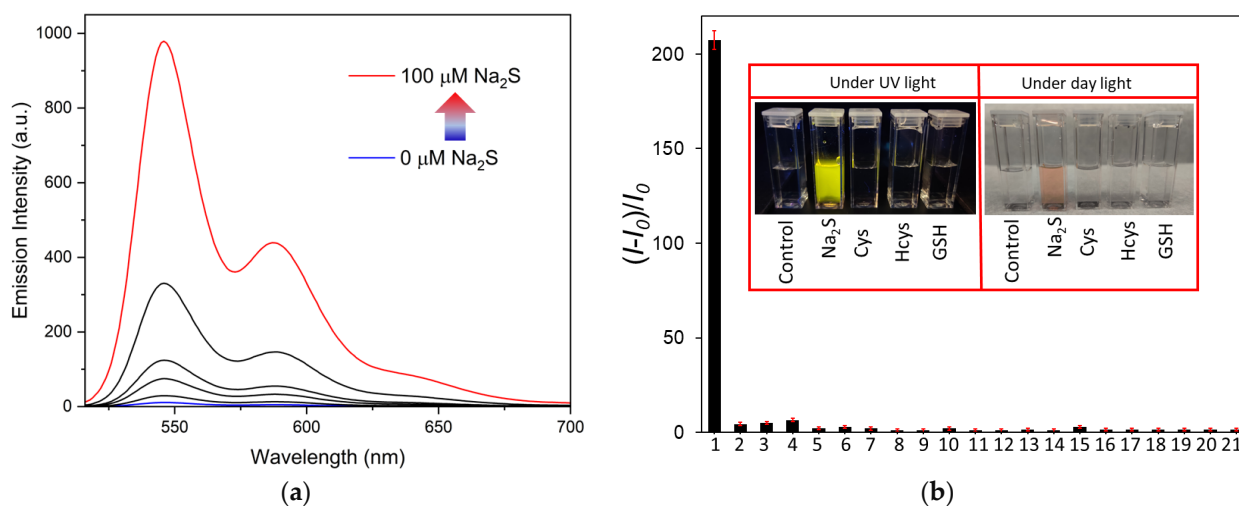

Figure 4. (**a**) Fluorescence turn-on response of **APBI-Cu** nanorods in presence of Na_2S (from 0–100 μM) in pure aqueous medium. (**b**) Relative fluorescence intensity change **APBI-Cu** nanorods toward various competitive analytes (100 μM) (1) Na_2S, (2) cysteine, (3) homocysteine, (4) glutathione, (5) NaF, (6) NaCl, (7) NaBr, (8) NaI, (9) $NaNO_2$, (10) $NaNO_3$, (11) $NaHSO_3$, (12) Na_2SO_3, (13) Na_2SO_4, (14) $NaHCO_3$, (15) Na_3PO_4, (16) ethanol, (17) hexanol, (18) phenol, (19) acetic acid, (20) butanoic acid and (21) hexanal Inset: naked eye visualization of the fluorometric and colorimetric change of **APBI-Cu** nanorods in the presence of Na_2S and other thiol containing biomolecules.

Different thiol-containing amino acids are one of the main sources of sulfide contamination in food and other biological samples [56–58]. In addition, the affinity of such thiol-containing amino acids towards copper ion is also high [59–61]. Thus, thiol-containing amino acids and other thiol containing biomolecules could show false positive responses. To test the selectivity towards sulfide over other interfering substances, **APBI-Cu** nanorods were treated with different thiol-containing biomolecules (cysteine (Cys), homocysteine (Hcys), glutathione (GSH)), various anions (NaF, NaCl, NaBr, NaI, $NaNO_3$, $NaNO_2$, $NaHSO_3$, NaS_2O_3, Na_2SO_4, $NaHCO_3$ and Na_3PO_4) and meat spoilage-associated volatile organic compounds (ethanol, hexanol, phenol, acetic acid, butanoic acid and hexanal) [62]. Figure 4b and Figure S6 and Supplementary Materials show that no strong response was found from other interfering substances. Concentration dependent fluorescence studies show that the **APBI-Cu** nanorods are capable enough to distinguish among sulfide and other interfering molecules and anions (Figure S7, Supplementary Materials). Thus, **APBI-Cu** nanorods are highly selective towards sulfide over common thiol containing biomolecules and various anions.

An efficient sensor must work in a complicated system where the target analyte coexists with other interfering substances. To check the sensitivity of **APBI-Cu** nanorods, another set of experiments was designed. Here, the interfering molecules and anions were added to an equal amount of sulfide. As shown in Figure 5 and Figures S8–S27, Supplementary Materials, a similar turn-on signal was observed from **APBI-Cu** nanorods and no strong interference was noticed even with other molecules present. Based on these results, we can conclude that the self-assembled **APBI-Cu** nanorods are not only selective towards sulfide, but also highly sensitive. Further, the limit of detection was calculated in the concentration range of 0–12 μM and the plot of the fluorescence intensity of **APBI-Cu** nanorods vs. the concentration of Na_2S revealed a linear relationship (Figure S28,

Supplementary Materials). The LOD for the detection of sulfide was calculated at a signal-to-noise (S/N) ratio of 3 and has been estimated to be 0.181 μM.
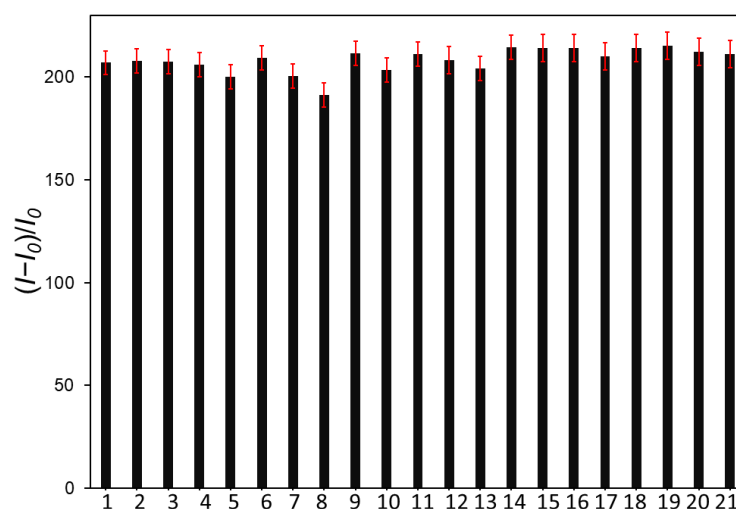

Figure 5. Bar plot showing relative fluorescence intensity change of **APBI-Cu** nanorods toward Na₂S in presence of various competitive analytes (100 μM) (1) no competitive analyte, (2) cysteine, (3) homocysteine, (4) glutathione, (5) NaF, (6) NaCl, (7) NaBr, (8) NaI, (9) NaNO₂, (10) NaNO₃, (11) NaHSO₃, (12) Na₂SO₃, (13) Na₂SO₄, (14) NaHCO₃, and (15) Na₃PO₄, (16) ethanol, (17) hexanol, (18) phenol, (19) acetic acid, (20) butanoic acid and (21) hexanal.

Metal ion displacement approach (MDA) is a common mechanism for sulfide sensors [63–65] (Table S1, Supplementary Materials). In the presence of sulfide, metals convert to metal sulfides. The fluorophore then shows turn-on signals as it is released in solution. As discussed earlier, we observed similar emission and absorption signals from **APBI-Cu** nanorods in the presence of sulfide. In addition, ^{1}H-NMR of **APBI-Cu** nanorods were recorded before and after the treatment of Na₂S in D₂O (Figures S29–S31, Supplementary Materials). No obvious peaks were found in ^{1}H-NMR for only **APBI-Cu** nanorods as they are insoluble in water. On the other hand, Na₂S treated **APBI-Cu** nanorods show a similar ^{1}H-NMR signal compered to free APBI-K [33]. The peaks at 7.96 and 8.02 ppm could be assigned to aromatic protons of the PDI core of APBI molecules. The peak around 3.14 ppm shifted to 2.65 ppm, which might occur from the different metal environments around the carboxylate functionalized molecule [66,67]. The SEM images of **APBI-Cu** nanorods were taken after the treatment of Na₂S to observe any changes in morphology. Figure S32, Supplementary Materials confirms that the nanorods lost their shape after the sensing event, which also supports the copper ion displacement mechanism. The detection mechanism is shown in Scheme 2.
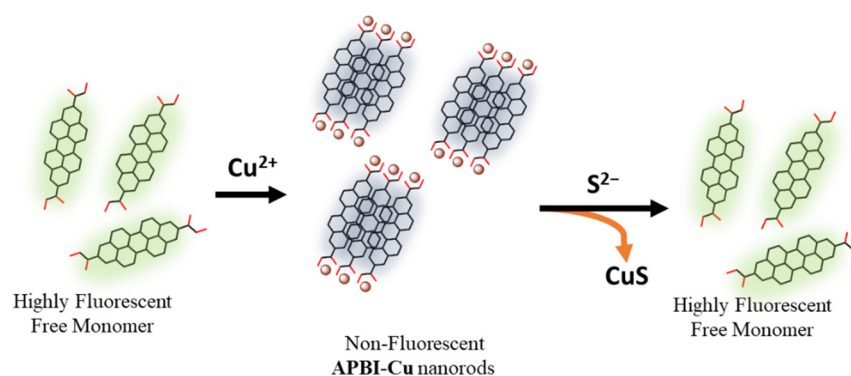
Scheme 2. Schematic presentation of detection of sulfide based on the **APBI-Cu** nanorods.

3.3. Detection of Sulfide in Water and Meat

'Sulfur bacteria' can produce toxic sulfide in groundwater, wells, and even plumbing [68,69]. Use or consumption of sulfide contaminated water is bad for human health. Considering the possible use of the **APBI-Cu** nanorods for on-site detection of sulfide without using any complex device, a paper test strip (~3 cm × 5 cm) was utilized. Paper strips were dipped in various concentrations of Na$_2$S solution made by laboratory tap water. The **APBI-Cu** nanorods-coated paper test strip showed gradually enhanced emission under UV lamp with increasing concentration from 0 μM to 100 μM (Figure 6). These observations indicate that the **APBI-Cu** nanorods coated paper can be used for the on-site detection of sulfide in water.
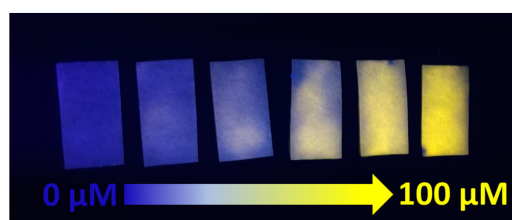
Figure 6. Digital images of paper strips coated with **APBI-Cu** under UV-lamp after the treatment of various concentrations of Na$_2$S made in tap water.

As it spoils, meat produces a high amount of sulfides via the degradation of proteins [70,71]. In such cases, sulfide can act as a marker of meat spoilage [72]. Chicken mince was kept at room temperature and another set of meat was stored at −4 °C. The collected gas from the headspace of the flask was slowly bubbled in the aqueous suspension of **APBI-Cu** nanorods. Emission spectra were then recorded. No remarkable turn-on signal was observed in the initial 2 days from both samples. A detectable turn-on signal was observed from the meat stored at room temperature after 3 days. As shown in Figure 7 and Figure S33, Supplementary Materials, the turn on signal increased with time. On the other hand, no turn-on signal was observed for the gas collected from the headspace of the chicken-containing flask stored at −4 °C, which indicates that the meat remained fresh and was not undergoing spoilage. No turn-on signal was observed when only air was bubbled in the aqueous suspension of **APBI-Cu** nanorods as a control experiment. In addition, when **APBI-Cu** nanorods coated paper was placed on fully spoiled meat, a rapid color change was observed with an enhanced fluorescence signal under UV-lamp (Figure S34, Supplementary Materials). These observations suggest that the **APBI-Cu** nanorods can be utilized as an indicator of raw meat freshness via monitoring the released sulfide from the meat sample.
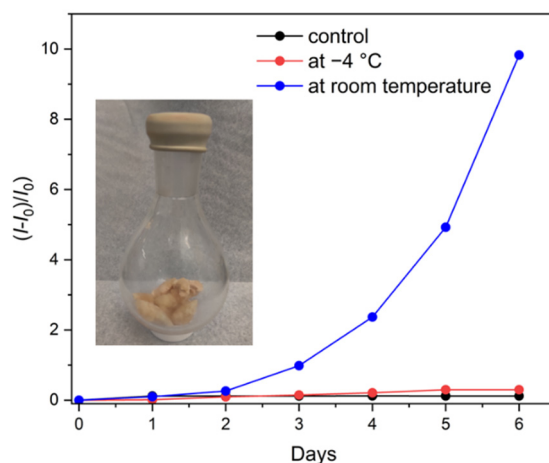

Figure 7. Relative fluorescence intensity changes of **APBI-Cu** nanorod sensor at different conditions

toward sulfide during a 6-day period of chicken meat spoilage process. Inset showing the round bottom flask used for storage of meat samples.

4. Conclusions

In short, an **APBI-Cu** nanorod based colorimetric and fluorometric probe was developed. The **APBI-Cu** nanorods can selectively detect the toxic sulfide without interference from common thiol-containing biomolecules like cysteine, homocysteine, and glutathione. Water soluble APBI molecules undergo controlled coordination-induced self-assembly with copper and show a fluorescent turn-off signal. In the presence of sulfide, **APBI-Cu** nanorods begin disassembling. This phenomenon was made evident by spectroscopic investigation, morphology evaluation, and observation of a distinct turn-on signal. The **APBI-Cu** nanorod probe showed sensitive and selective detection of sulfide with a low detection limit of 0.181 μM in a purely aqueous medium, which is significantly lower than those reported recently with other perylene diimide fluorescent probes. Finally, it has been successfully utilized to detect sulfide in both water and meat samples. Hence, this newly developed colorimetric and fluorometric sulfide sensor has great potential in the fields of water and meat spoilage monitoring.

(a) daylight and (b) UV-lamp before and after the contact with spoiled meat; Table S1: List of few recently reported sulfide sensor material works with similar metal ion displacement mechanism. References [2,30–32,49–55,73–80] are cited in the supplementary materials.

References

1. Jiang, J.; Chan, A.; Ali, S.; Saha, A.; Haushalter, K.J.; Lam, W.-L.M.; Glasheen, M.; Parker, J.; Brenner, M.; Mahon, S.B. Hydrogen sulfide—Mechanisms of toxicity and development of an antidote. *Sci. Rep.* **2016**, *6*, 20831. [CrossRef]
2. Ren, M.; Xu, Q.; Bai, Y.; Wang, S.; Kong, F. Construction of a dual-response fluorescent probe for copper (II) ions and hydrogen sulfide (H2S) detection in cells and its application in exploring the increased copper-dependent cytotoxicity in present of H2S. *Spectrochim. Acta Part A* **2021**, *249*, 119299. [CrossRef]
3. Chu, L.; Dong, Z.; Xu, X.; Cochran, D.L.; Ebersole, J.L. Role of glutathione metabolism of Treponema denticola in bacterial growth and virulence expression. *Infect. Immun.* **2002**, *70*, 1113–1120. [CrossRef]
4. Zheng, Y.; Yu, B.; De La Cruz, L.K.; Roy Choudhury, M.; Anifowose, A.; Wang, B. Toward hydrogen sulfide based therapeutics: Critical drug delivery and developability issues. *Med. Res. Rev.* **2018**, *38*, 57–100. [CrossRef]
5. Powell, C.R.; Dillon, K.M.; Matson, J.B. A review of hydrogen sulfide (H2S) donors: Chemistry and potential therapeutic applications. *Biochem. Pharmacol.* **2018**, *149*, 110–123. [CrossRef]
6. Panagaki, T.; Randi, E.B.; Augsburger, F.; Szabo, C. Overproduction of H2S, generated by CBS, inhibits mitochondrial Complex IV and suppresses oxidative phosphorylation in Down syndrome. *Proc. Natl. Acad. Sci. USA* **2019**, *116*, 18769–18771. [CrossRef]
7. Zhao, H.; Liu, H.; Yang, Y.; Wang, H. The Role of H2S Regulating NLRP3 Inflammasome in Diabetes. *Int. J. Mol. Sci.* **2022**, *23*, 4818. [CrossRef]
8. Fiorucci, S.; Antonelli, E.; Mencarelli, A.; Orlandi, S.; Renga, B.; Rizzo, G.; Distrutti, E.; Shah, V.; Morelli, A. The third gas: H2S regulates perfusion pressure in both the isolated and perfused normal rat liver and in cirrhosis. *Hepatology* **2005**, *42*, 539–548. [CrossRef]
9. Guidotti, T.L. Hydrogen sulfide: Advances in understanding human toxicity. *Int. J. Toxicol.* **2010**, *29*, 569–581. [CrossRef]
10. Huang, H.; Li, M.; Hao, M.; Yu, L.L.; Li, Y. A novel selective detection method for sulfide in food systems based on the GMP-Cu nanozyme with laccase activity. *Talanta* **2021**, *235*, 122775. [CrossRef]
11. Singh, S.; Shin, Y.; Lee, Y.S. Antimicrobial seafood packaging: A review. *J. Food Sci. Technol.* **2016**, *53*, 2505–2518. [CrossRef] [PubMed]
12. Yang, X.; Lu, X.; Wang, J.; Zhang, Z.; Du, X.; Zhang, J.; Wang, J. Near-infrared fluorescent probe with a large Stokes shift for detection of hydrogen sulfide in food spoilage, living cells, and zebrafish. *J. Agric. Food Chem.* **2022**, *70*, 3047–3055. [CrossRef] [PubMed]
13. Zhai, X.; Li, Z.; Shi, J.; Huang, X.; Sun, Z.; Zhang, D.; Zou, X.; Sun, Y.; Zhang, J.; Holmes, M. A colorimetric hydrogen sulfide sensor based on gellan gum-silver nanoparticles bionanocomposite for monitoring of meat spoilage in intelligent packaging. *Food Chem.* **2019**, *290*, 135–143. [CrossRef]
14. Lynch, M.J.; Crane, B.R. Design, validation, and application of an enzyme-coupled hydrogen sulfide detection assay. *Biochemistry* **2018**, *58*, 474–483. [CrossRef]
15. Jarosz, A.P.; Yep, T.; Mutus, B. Microplate-based colorimetric detection of free hydrogen sulfide. *Anal. Chem.* **2013**, *85*, 3638–3643. [CrossRef] [PubMed]
16. Khan, M.A.; Qazi, F.; Hussain, Z.; Idrees, M.U.; Soomro, S.; Soomro, S. Recent trends in electrochemical detection of NH3, H2S and NOx gases. *Int. J. Electrochem. Sci.* **2017**, *12*, 1711–1733. [CrossRef]

17. Zhao, Y.; Yang, Y.; Cui, L.; Zheng, F.; Song, Q. Electroactive Au@ Ag nanoparticles driven electrochemical sensor for endogenous H2S detection. *Biosens. Bioelectron.* **2018**, *117*, 53–59. [CrossRef]

18. Govardhan, K.; Grace, A.N. Metal/metal oxide doped semiconductor based metal oxide gas sensors—A review. *Sens. Lett.* **2016**, *14*, 741–750. [CrossRef]

19. Ghimbeu, C.M.; Lumbreras, M.; Schoonman, J.; Siadat, M. Electrosprayed metal oxide semiconductor films for sensitive and selective detection of hydrogen sulfide. *Sensors* **2009**, *9*, 9122–9132. [CrossRef]

20. Du, J.; Wang, J.; Huang, W.; Deng, Y.; He, Y. Visible light-activatable oxidase mimic of 9-mesityl-10-methylacridinium ion for colorimetric detection of biothiols and logic operations. *Anal. Chem.* **2018**, *90*, 9959–9965. [CrossRef]

21. Fernandes, G.M.; Silva, W.R.; Barreto, D.N.; Lamarca, R.S.; Gomes, P.C.F.L.; da Petruci, S.J.F.; Batista, A.D. Novel approaches for colorimetric measurements in analytical chemistry–A review. *Anal. Chim. Acta* **2020**, *1135*, 187–203. [CrossRef]

22. Kaushik, R.; Ghosh, A.; Singh, A.; Jose, D.A. Colorimetric sensor for the detection of H2S and its application in molecular half-subtractor. *Anal. Chim. Acta* **2018**, *1040*, 177–186. [CrossRef] [PubMed]

23. Das, S.; Sahoo, P. A colorimetric sensor for hydrogen sulfide: Detection from biogas and quantitative estimation in water. *Sens. Actuators B* **2019**, *291*, 287–292. [CrossRef]

24. Cho, S.H.; Suh, J.M.; Eom, T.H.; Kim, T.; Jang, H.W. Colorimetric sensors for toxic and hazardous gas detection: A review. *Electron. Mater. Lett.* **2021**, *17*, 1–17. [CrossRef]

25. Kang, S.; Oh, J.; Han, M.S. A colorimetric sensor for hydrogen sulfide detection using direct inhibition of active site in G-quadruplex DNAzyme. *Dyes Pigm.* **2017**, *139*, 187–192. [CrossRef]

26. Sen, A.; Albarella, J.D.; Carey, J.R.; Kim, P.; McNamara III, W.B. Low-cost colorimetric sensor for the quantitative detection of gaseous hydrogen sulfide. *Sens. Actuators B* **2008**, *134*, 234–237. [CrossRef]

27. Alyan, A.K.; Hanafi, R.S.; Gad, M.Z. Point-of-care testing and optimization of sample treatment for fluorometric determination of hydrogen sulphide in plasma of cardiovascular patients. *J. Adv. Res.* **2021**, *27*, 1–10. [CrossRef]

28. Chemchem, M.; Chemchem, A.; Aydıner, B.; Seferoğlu, Z. Recent advances in colorimetric and fluorometric sensing of neurotransmitters by organic scaffolds. *Eur. J. Med. Chem.* **2022**, *244*, 114820. [CrossRef]

29. Yu, X.; Gong, Y.; Ji, H.; Cheng, C.; Lv, C.; Zhang, Y.; Zang, L.; Zhao, J.; Che, Y. Rapid Assessment of Meat Freshness by the Differential Sensing of Organic Sulfides Emitted during Spoilage. *ACS Sens.* **2022**, *7*, 1395–1402. [CrossRef]

30. Hou, F.; Cheng, J.; Xi, P.; Chen, F.; Huang, L.; Xie, G.; Shi, Y.; Liu, H.; Bai, D.; Zeng, Z. Recognition of copper and hydrogen sulfide in vitro using a fluorescein derivative indicator. *Dalton Trans.* **2012**, *41*, 5799–5804. [CrossRef]

31. Wu, S.; Ma, X.; Wang, Y.; Zhou, J.; Li, X.; Wang, X. A novel fluorescent BODIPY-based probe for detection of Cu2+ and H2S based on displacement approach. *Spectrochim. Acta Part A* **2021**, *249*, 119330. [CrossRef] [PubMed]

32. Strianese, M.; Guarnieri, D.; Lamberti, M.; Landi, A.; Peluso, A.; Pellecchia, C. Fluorescent salen-type Zn (II) complexes as probes for detecting hydrogen sulfide and its anion: Bioimaging applications. *Inorg. Chem.* **2020**, *59*, 15977–15986. [CrossRef]

33. Liu, Y.; Gao, X.; Zhao, M.; Lu, F.; Zheng, L. Formation of supermolecular chiral gels from L-aspartic acid-based perylenebisimides and benzene dicarboxylic acids. *New J. Chem.* **2017**, *41*, 7643–7649. [CrossRef]

34. Guo, L.; Panderi, I.; Yan, D.D.; Szulak, K.; Li, Y.; Chen, Y.-T.; Ma, H.; Niesen, D.B.; Seeram, N.; Ahmed, A. A comparative study of hollow copper sulfide nanoparticles and hollow gold nanospheres on degradability and toxicity. *ACS Nano* **2013**, *7*, 8780–8793. [CrossRef] [PubMed]

35. Powell, C.R.; Dillon, K.M.; Wang, Y.; Carrazzone, R.J.; Matson, J.B. A persulfide donor responsive to reactive oxygen species: Insights into reactivity and therapeutic potential. *Angew. Chem. Int. Ed.* **2018**, *130*, 6432–6436. [CrossRef]

36. Zhang, F.; Ma, Y.; Chi, Y.; Yu, H.; Li, Y.; Jiang, T.; Wei, X.; Shi, J. Self-assembly, optical and electrical properties of perylene diimide dyes bearing unsymmetrical substituents at bay position. *Sci. Rep.* **2018**, *8*, 8208. [CrossRef]

37. Chen, S.; Slattum, P.; Wang, C.; Zang, L. Self-assembly of perylene imide molecules into 1D nanostructures: Methods, morphologies, and applications. *Chem. Rev.* **2015**, *115*, 11967–11998. [CrossRef]

38. Datar, A.; Balakrishnan, K.; Zang, L. One-dimensional self-assembly of a water soluble perylene diimide molecule by pH triggered hydrogelation. *Chem. Commun.* **2013**, *49*, 6894–6896. [CrossRef]

39. Pramanik, B.; Ahmed, S.; Singha, N.; Das, D. Self-Assembly Assisted Tandem Sensing of Pd2+ and CN− by a Perylenediimide-Peptide Conjugate. *ChemistrySelect* **2017**, *2*, 10061–10066. [CrossRef]

40. Muthuraj, B.; Chowdhury, S.R.; Mukherjee, S.; Patra, C.R.; Iyer, P.K. Aggregation deaggregation influenced selective and sensitive detection of Cu 2+ and ATP by histidine functionalized water-soluble fluorescent perylene diimide under physiological conditions and in living cells. *RSC Adv.* **2015**, *5*, 28211–28218. [CrossRef]

41. Feng, X.; An, Y.; Yao, Z.; Li, C.; Shi, G. A turn-on fluorescent sensor for pyrophosphate based on the disassembly of Cu2+-mediated perylene diimide aggregates. *ACS Appl. Mater. Interfaces* **2012**, *4*, 614–618. [CrossRef] [PubMed]

42. Balakrishnan, K.; Datar, A.; Naddo, T.; Huang, J.; Oitker, R.; Yen, M.; Zhao, J.; Zang, L. Effect of side-chain substituents on self-assembly of perylene diimide molecules: Morphology control. *J. Am. Chem. Soc.* **2006**, *128*, 7390–7398. [CrossRef]

43. Dalapati, R.; Balaji, S.; Trivedi, V.; Khamari, L.; Biswas, S. A dinitro-functionalized Zr (IV)-based metal-organic framework as colorimetric and fluorogenic probe for highly selective detection of hydrogen sulphide. *Sens. Actuators B* **2017**, *245*, 1039–1049. [CrossRef]

44. Sheals, J.; Persson, P.; Hedman, B. IR and EXAFS spectroscopic studies of glyphosate protonation and copper (II) complexes of glyphosate in aqueous solution. *Inorg. Chem.* **2001**, *40*, 4302–4309. [CrossRef] [PubMed]

45. Karaliota, A.; Kretsi, O.; Tzougraki, C. Synthesis and characterization of a binuclear coumarin-3-carboxylate copper (II) complex. *J. Inorg. Biochem.* **2001**, *84*, 33–37. [CrossRef] [PubMed]

46. Hao, Y.; Chen, W.; Wang, L.; Zhu, X.; Zhang, Y.; Qu, P.; Liu, L.; Zhou, B.; Liu, Y.-N.; Xu, M. A retrievable, water-soluble and biocompatible fluorescent probe for recognition of Cu (II) and sulfide based on a peptide receptor. *Talanta* **2015**, *143*, 307–314. [CrossRef]

47. Li, Y.; Wang, L.-J.; Fan, H.-L.; Shangguan, J.; Wang, H.; Mi, J. Removal of sulfur compounds by a copper-based metal organic framework under ambient conditions. *Energy Fuels* **2015**, *29*, 298–304. [CrossRef]

48. Abdel-Gawwad, H.A.; Hussein, H.; Mohammed, M.S. Bio-removal of Pb, Cu, and Ni from solutions as nano-carbonates using a plant-derived urease enzyme–urea mixture. *Environ. Sci. Pollut. Res.* **2020**, *27*, 30741–30754. [CrossRef]

49. Han, X.; Gu, C.; Ding, Y.; Yu, J.; Li, K.; Zhao, D.; Chen, B. Stable Eu3+/Cu2+-functionalized supramolecular Zinc (II) complexes as fluorescent probes for turn-on and ratiometric detection of hydrogen sulfide. *ACS Appl. Mater. Interfaces* **2021**, *13*, 20371–20379. [CrossRef]

50. Kaushik, R.; Sakla, R.; Ghosh, A.; Selvan, G.T.; Selvakumar, P.M.; Jose, D.A. Selective detection of H2S by copper complex embedded in vesicles through metal indicator displacement approach. *ACS Sens.* **2018**, *3*, 1142–1148. [CrossRef]

51. Lou, X.; Mu, H.; Gong, R.; Fu, E.; Qin, J.; Li, Z. Displacement method to develop highly sensitive and selective dual chemosensor towards sulfide anion. *Analyst* **2011**, *136*, 684–687. [CrossRef] [PubMed]

52. Hu, Y.; Yin, J.; Yoon, J. A multi-responsive cyanine-based colorimetric chemosensor containing dipicolylamine moieties for the detection of Zn (II) and Cu (II) ions. *Sens. Actuators B* **2016**, *230*, 40–45. [CrossRef]

53. Gao, X.; Li, Y.; Zhang, J.; Cheng, N.; Zhang, L.; Zhang, Z.; Yao, Z. Rapid detection of hydrogen sulfide in vegetables and monosodium glutamate based on perylene supramolecular aggregates using an indicator displacement assays strategy. *Spectrochim. Acta Part A* **2022**, *276*, 121223. [CrossRef] [PubMed]

54. Palanisamy, S.; Lee, L.-Y.; Wang, Y.-L.; Chen, Y.-J.; Chen, C.-Y.; Wang, Y.-M. A water soluble and fast response fluorescent turn-on copper complex probe for H2S detection in zebra fish. *Talanta* **2016**, *147*, 445–452. [CrossRef]

55. Zheng, X.; Fan, R.; Song, Y.; Xing, K.; Wang, P.; Yang, Y. Dual-Emitting Eu (III)–Cu (II) heterometallic–organic framework: Simultaneous, selective, and sensitive detection of hydrogen sulfide and ascorbic acid in a wide range. *ACS Appl. Mater. Interfaces* **2018**, *10*, 32698–32706. [CrossRef]

56. Ciccone, V.; Genah, S.; Morbidelli, L. Endothelium as a source and target of H2S to improve its trophism and function. *Antioxidants* **2021**, *10*, 486. [CrossRef]

57. Yang, Q.; He, G.-W. Imbalance of homocysteine and H2S: Significance, mechanisms, and therapeutic promise in vascular injury. *Oxid. Med. Cell. Longevity* **2019**, *2019*, 11. [CrossRef]

58. Yu, Y.; Li, G.; Wu, D.; Zheng, F.; Zhang, X.; Liu, J.; Hu, N.; Wang, H.; Wu, Y. Determination of hydrogen sulfide in wines based on chemical-derivatization-triggered aggregation-induced emission by high-performance liquid chromatography with fluorescence detection. *J. Agric. Food Chem.* **2019**, *68*, 876–883. [CrossRef]

59. Yoshinari, N.; Kuwamura, N.; Kojima, T.; Konno, T. Development of coordination chemistry with thiol-containing amino acids. *Coord. Chem. Rev.* **2023**, *474*, 214857. [CrossRef]

60. Abdollahiyan, P.; Hasanzadeh, M.; Seidi, F.; Pashazadeh-Panahi, P. An innovative colorimetric platform for the low-cost and selective identification of Cu (II), Fe (III), and Hg (II) using GQDs-DPA supported amino acids by microfluidic paper-based (µPADs) device: Multicolor plasmonic patterns. *J. Environ. Chem. Eng.* **2021**, *9*, 106197. [CrossRef]

61. Pang, X.; Gao, L.; Feng, H.; Li, X.; Kong, J.; Li, L. A peptide-based multifunctional fluorescent probe for Cu 2+, Hg 2+ and biothiols. *New J. Chem.* **2018**, *42*, 15770–15777. [CrossRef]

62. Mansur, A.R.; Seo, D.-H.; Song, E.-J.; Song, N.-E.; Hwang, S.H.; Yoo, M.; Nam, T.G. Identifying potential spoilage markers in beef stored in chilled air or vacuum packaging by HS-SPME-GC-TOF/MS coupled with multivariate analysis. *LWT* **2019**, *112*, 108256. [CrossRef]

63. Kaushik, R.; Ghosh, A.; Jose, D.A. Recent progress in hydrogen sulphide (H2S) sensors by metal displacement approach. *Coord. Chem. Rev.* **2017**, *347*, 141–157. [CrossRef]

64. Ibrahim, H.; Serag, A.; Farag, M.A. Emerging analytical tools for the detection of the third gasotransmitter H2S, a comprehensive review. *J. Adv. Res.* **2021**, *27*, 137–153. [CrossRef] [PubMed]

65. Jose, D.A.; Sharma, N.; Sakla, R.; Kaushik, R.; Gadiyaram, S. Fluorescent nanoprobes for the sensing of gasotransmitters hydrogen sulfide (H2S), nitric oxide (NO) and carbon monoxide (CO). *Methods* **2019**, *168*, 62–75. [CrossRef] [PubMed]

66. Bukhari, S.B.; Memon, S.; Mahroof-Tahir, M.; Bhanger, M. Synthesis, characterization and antioxidant activity copper–quercetin complex. *Spectrochim. Acta Part A* **2009**, *71*, 1901–1906. [CrossRef]

67. Etaiw, S.E.d.H.; El-bendary, M.M. Crystal structure, characterization and catalytic activities of Cu (II) coordination complexes with 8-hydroxyquinoline and pyrazine-2-carboxylic acid. *Appl. Organomet. Chem.* **2018**, *32*, e4213. [CrossRef]

68. Lloyd, D. Hydrogen sulfide: Clandestine microbial messenger? *Trends Microbiol.* **2006**, *14*, 456–462. [CrossRef]

69. Li, Y.; Alaimo, C.P.; Kim, M.; Kado, N.Y.; Peppers, J.; Xue, J.; Wan, C.; Green, P.G.; Zhang, R.; Jenkins, B.M. Composition and toxicity of biogas produced from different feedstocks in California. *Environ. Sci. Technol.* **2019**, *53*, 11569–11579. [CrossRef]

70. Li, H.; Geng, W.; Sun, X.; Wei, W.; Mu, X.; Ahmad, W.; Hassan, M.M.; Ouyang, Q.; Chen, Q. Fabricating a nano-bionic sensor for rapid detection of H2S during pork spoilage using Ru NPs modulated catalytic hydrogenation conversion. *Meat Sci.* **2021**, *177*, 108507. [CrossRef]

71. Dave, D.; Ghaly, A.E. Meat spoilage mechanisms and preservation techniques: A critical review. *Am. J. Agric. Biol. Sci.* **2011**, *6*, 486–510. [CrossRef]

72. Lin, Y.; Zhan, Y.; Luo, F.; Lin, C.; Wang, J.; Qiu, B.; Lin, Z. Multicolor hydrogen sulfide sensor for meat freshness assessment based on Cu2+-modified boron nitride nanosheets-supported subnanometer gold nanoparticles. *Food Chem.* **2022**, *381*, 132278. [CrossRef]

73. Dong, Z.; Le, X.; Zhou, P.; Dong, C.; Ma, J. Sequential recognition of zinc ion and hydrogen sulfide by a new quinoline derivative with logic gate behavior. *RSC Adv.* **2014**, *4*, 18270–18277. [CrossRef]

74. Gao, L.-L.; Wang, B.-B.; Chen, X.; Wang, Y.; Wu, W.-N.; Zhao, X.-L.; Yan, L.-L.; Fan, Y.-C.; Xu, Z.-H. Hydrazone derivative bearing coumarin for the relay detection of Cu2+ and H2S in an almost neat aqueous solution and bioimaging in lysosomes. *Spectrochim. Acta Part A* **2021**, *255*, 119693. [CrossRef]

75. Liu, B.; Chen, Y. Responsive lanthanide coordination polymer for hydrogen sulfide. *Anal. Chem.* **2013**, *85*, 11020–11025. [CrossRef] [PubMed]

76. Chen, J.; Li, Y.; Lv, K.; Zhong, W.; Wang, H.; Wu, Z.; Yi, P.; Jiang, J. Cyclam-functionalized carbon dots sensor for sensitive and selective detection of copper (II) ion and sulfide anion in aqueous media and its imaging in live cells. *Sens. Actuators B* **2016**, *224*, 298–306. [CrossRef]

77. Wang, Z.-X.; Zheng, C.-L.; Ding, S.-N. Label-free detection of sulfide ions based on fluorescence quenching of unmodified core–shell Au@ Ag nanoclusters. *RSC Adv.* **2014**, *4*, 9825–9829. [CrossRef]

78. Barati, A.; Shamsipur, M.; Abdollahi, H. Metal-ion-mediated fluorescent carbon dots for indirect detection of sulfide ions. *Sens. Actuators B* **2016**, *230*, 289–297. [CrossRef]

79. Hai, Z.; Bao, Y.; Miao, Q.; Yi, X.; Liang, G. Pyridine–biquinoline–metal complexes for sensing pyrophosphate and hydrogen sulfide in aqueous buffer and in cells. *Anal. Chem.* **2015**, *87*, 2678–2684. [CrossRef]

80. Dong, Z.; Le, X.; Zhou, P.; Dong, C.; Ma, J. An "off–on–off" fluorescent probe for the sequential detection of Zn 2+ and hydrogen sulfide in aqueous solution. *New J. Chem.* **2014**, *38*, 1802–1808. [CrossRef]